Vertex functions and infrared fixed point in Landau gauge SU(N) Yang-Mills theory

R. Alkofer[1], C. S. Fischer[2], F. J. Llanes-Estrada[3]

[1]*Institute for Theoretical Physics, U. Tübingen, D-72076 Tübingen, Germany*
[2]*IPPP, University of Durham, Durham DH1 3LE, U.K.*
[3]*Dept. Física Teorica I, Univ. Complutense, Madrid 28040, Spain*

Abstract

The infrared behaviour of vertex functions in an $SU(N)$ Yang-Mills theory in Landau gauge is investigated employing a skeleton expansion of the Dyson-Schwinger equations. The three- and four-gluon vertices become singular if and only if all external momenta vanish while the dressing of the ghost-gluon vertex remains finite in this limit. The running coupling as extracted from either of these vertex functions possesses an infrared fixed point. In general, diagrams including ghost-loops dominate in the infrared over purely gluonic ones.

Key words: Confinement, Universality, Non-perturbative QCD, Running coupling, Dyson-Schwinger equations, Infrared behaviour.
PACS: 12.38.Aw 14.70.Dj 12.38.Lg 11.15.Tk 02.30.Rz

Fifty years after the formulation of Yang-Mills theory its infrared (IR) structure is still largely unknown despite the fact that this knowledge is central to any effort in understanding the strong interactions from first principles. It has long been conjectured that IR enhancements are present. Indeed they are necessary to explain confinement. Such IR enhancements may also be the reason that no explicit glue becomes visible in the low-lying hadron mass spectrum.

Lattice calculations include in principle all non-perturbative features of Yang-Mills theories but are in practice limited by the finite lattice volume in the study of possible IR singularities [1,2,3,4]. A complementary non-perturbative continuum method is provided by the Dyson-Schwinger equations (DSEs). In Landau gauge the DSEs for the ghost and gluon propagators have been analytically solved in the IR assuming ghost dominance [5,6,7,8,9,10,11]. Lattice and DSEs are complementary and yet they agree on the propagators' IR behaviour: there is clear evidence for an IR finite or even vanishing gluon propagator and a strongly diverging ghost propagator, in accordance with both, the Kugo-Ojima confinement criterion [12] and the Gribov-Zwanziger scenario [13].

The running of the gauge coupling is intimately related to the momentum dependence of the primitively divergent vertex functions in an $SU(N_c)$ Yang-Mills theory. For sufficiently large momenta the coupling can be calculated from perturbative corrections to these vertex functions [14]. The breakdown of perturbation theory is signaled by Landau poles, unphysical singularities at non-vanishing space-like momenta. By simply imposing analyticity for space-like momenta extrapolations to the IR have been performed in so-called Analytic Perturbation Theory [15,16,17]. Typically these studies find a well-behaved coupling at all momenta and an IR fixed point. Qualitatively this agrees with the findings from the genuinely non-perturbative continuum approaches. In the latter the IR behavior of the ghost-gluon interaction in Landau gauge has been determined either from DSEs or the Exact Renormalization Group Equations (ERGEs) [8,9,18,19] and yield an IR fixed point with $\alpha(0) \approx 8.9/N_c$. The corresponding couplings from the three- and four-gluon vertex functions have not yet been studied with these techniques. Within perturbation theory the principle of gauge invariance leads to the universality of the gauge coupling: All three couplings are equal up to the well-known renormalization scheme dependencies [14,20,21] at every finite order. Although a general proof is lacking one expects such relations to also hold in the full non-perturbative theory.

In this letter we propose a method to investigate the IR behaviour of Greens functions with an arbitrary number of ghosts and gluons. We detail the results for the gluon-self interaction vertices thus completing our knowledge about the primitively divergent vertex functions (*i.e.* those appearing in the renormalized Lagrangian) and the corresponding running coupling(s) in the deep IR. We construct a skeleton expansion for each DSE employing the fully dressed primitively divergent n-point functions of Yang-Mills theory. To all orders in this expansion the three- and four-gluon vertex functions are IR singular if and only if all external momenta vanish. The corresponding IR exponents are hereby proportional to the IR exponent of the ghost renormalization function such that the corresponding couplings have IR fixed points. The results presented in this letter verify the self-consistency of ghost dominance in a quite general way and prove that ghost dominance is a successful guiding principle when determining the IR behaviour of Yang-Mills Greens functions in the confining phase.

In Landau gauge, the ghost and gluon propagators in Euclidean momentum space are described by the renormalization functions $G(p^2)$ and $Z(p^2)$:

$$D^G(p^2) = -\frac{G(p^2)}{p^2}, \qquad D_{\mu\nu}(p^2) = \left(\delta_{\mu\nu} - \frac{p_\mu p_\nu}{p^2}\right)\frac{Z(p^2)}{p^2}. \qquad (1)$$

On the other hand, the three- and four-point functions feature tensor structures not present in the bare Lagrangian thus requiring multiple such scalar

functions. We will not specify these yet and discuss first the behaviour of the scalar amplitude multiplying only the tensor defined on the level of the bare Lagrangian. *E.g.* for the three-gluon vertex this tensor reads

$$\delta_{\mu_1\mu_2}(p_1 - p_2)_{\mu_3} + \delta_{\mu_2\mu_3}(p_2 - p_3)_{\mu_1} + \delta_{\mu_3\mu_1}(p_3 - p_1)_{\mu_2} \,. \tag{2}$$

In a setting where all external momenta $(p_i)^2$ vanish as a single momentum scale $p^2 \to 0$ this tensor will be multiplied by an amplitude $H_1^{3g}(p^2)$ in the fully dressed three-gluon vertex. For the four-gluon and ghost-gluon vertex functions the amplitudes $H_1^{4g}(p^2)$ and $H_1^{gh-g}(p^2)$ are defined analogously. Starting from the established result [8,9,18,19]

$$Z(p^2) \to (p^2)^{2\kappa} \,, \qquad G(p^2) \to (p^2)^{-\kappa} \,, \tag{3}$$

we will show in the following that for $p^2 \to 0$

$$H_1^{3g}(p^2) \to (p^2)^{-3\kappa} \,, \qquad H_1^{4g}(p^2) \to (p^2)^{-4\kappa} \,, \qquad H_1^{gh-g}(p^2) \to \text{const.} \tag{4}$$

where the parameter κ is determined from the propagator DSEs, see below. Eqs. (3) imply that the minimum of a gluon's dispersion relation does not occur at zero momentum.[1] In addition, it concurs with Zwanziger's picture [13]: the geometric degrees of freedom dominate IR Yang-Mills theory. Eqs. (4), on the other hand, state that the self-interactions of gluons become large at very low momentum. The connected three- and four-gluon functions hereby violate the bound conjectured in ref. [23], although only at one specific kinematical point.

It will be demonstrated in the following that each of the eqs. (3) and (4) is correct when the others are assumed as given. At the end, one thus obtains a self-consistent solution of the DSE system in the IR. The starting point is provided by the observation that in Landau gauge the ghost-gluon vertex is UV finite and remains bare for vanishing incoming ghost momentum [24,25]. This is easily shown using the DSE for the full ghost-gluon vertex, see fig. 1. The bare ghost-gluon vertex in the interaction diagram is proportional to the internal loop momenum l_μ. Due to the transversality of the gluon propagator $D_{\mu\nu}$ one has $l_\mu D_{\mu\nu}(l-q) = q_\mu D_{\mu\nu}(l-q)$. Thus, the interaction diagram vanishes for $q_\mu \to 0$. This argument would only be invalidated if the two-ghost–two-gluon scattering kernel had an IR divergence. However, recent lattice results and numerical DSE studies of the ghost-gluon vertex [26,27] agree with a bare vertex in the IR. From our analytical study it also follows that such a divergence is absent.

The IR behaviour of two-point functions has been adressed within ERGEs and DSEs [6,7,8,9,10,18,19]. We briefly discuss the IR aspects of the ghost propagator DSE depicted in fig. 2. With an IR finite ghost-gluon vertex, see

---

[1] The phenomenological consequences of an IR suppressed gluon propagator can for example be infered from ref. [22].
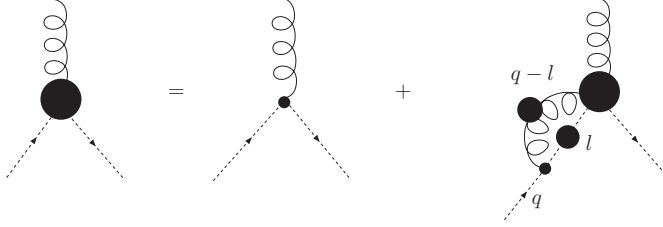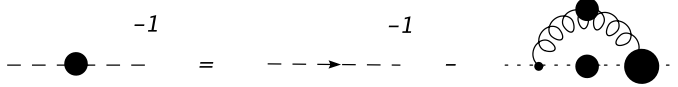
Fig. 1. Ghost-gluon vertex DSE.

Fig. 2. Ghost propagator DSE.

the last of eqs. (4), and a power law ansatz for the dressing functions at low external p^2, $Z(p^2) = A\,(p^2)^\alpha$ and $G(p^2) = B\,(p^2)^\beta$, a self-consistent solution arises with $\kappa := -\beta = 2\alpha$ from matching the exponents of both sides of the ghost DSE [28]. Hereby the formula for a scalar integral in d dimensions, depending on one external momentum p_μ

$$\int d^d q (q^2)^a ((q-p)^2)^b = (p^2)^{d/2+a+b} \frac{\Gamma(d/2+a)\Gamma(d/2+b)\Gamma(-a-b-d/2)}{\pi^2 \Gamma(-a)\Gamma(-b)\Gamma(d+a+b)} \quad (5)$$

has been used. The actual value of κ follows from IR consistency of the ghost with the gluon propagator DSE, and depends slightly on the details of the ghost-gluon vertex' (finite) dressing [9]. For a bare vertex one obtains $\kappa = (93 - \sqrt{1201})/98 \approx 0.595$. Note, however, that the precise value of κ will be irrelevant for all arguments presented in the following as long as $0 < \kappa < 1$ [9,28] and $\kappa \neq 1/2$ [9].

In a first step we establish the three-gluon vertex power law in eq. (4). The corresponding DSE (see fig. 3) includes four- and five-point functions which we treat in a skeleton expansion in terms of the fully dressed, primitively divergent Greens functions. Furthermore, we develop counting rules for the IR degree of divergence of a diagram. To lowest order in the expansion we can identify each subdiagram with its leading IR singularity. We will demonstrate that all higher order diagrams are either equally or less IR singular. If the three momenta entering the vertex are much smaller than Λ_{QCD} the integral will be dominated by loop momenta also smaller than Λ_{QCD} due to the denominators of the propagators. The dressing functions of these propagators are then the simple power laws given in eqs. (3), allowing to integrate the loops analytically. The ghost-loop diagram (a) in fig. 3 is IR leading. We thus evaluate this diagram first and then substitute the resulting power law for the three-gluon vertex into the other diagrams to check for self-consistency. This is simplest
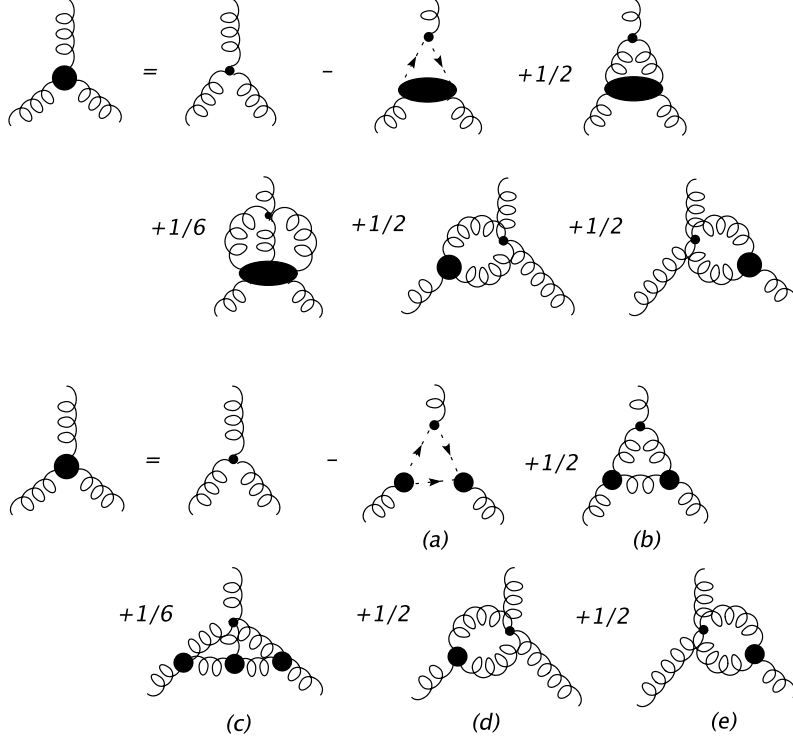
4

Fig. 3. Exact Dyson-Schwinger equation for the three-gluon vertex and lowest order in a skeleton expansion of the four- and five-point functions. All internal propagators in the diagrams are to be understood as fully dressed.

demonstrated at the symmetric kinematical point

$$p_1^2 = p_2^2 = p_3^2 = p^2, \qquad (p_1 \cdot p_2) = (p_1 \cdot p_3) = (p_2 \cdot p_3) \equiv -\frac{1}{2}p^2. \qquad (6)$$

The tensor structure of the three-gluon vertex then reduces from fourteen tensors at general kinematics to three independent ones [14]. Omitting the overall color factor and the delta function expressing momentum conservation the vertex is then given by

$$
\begin{aligned}
\Gamma_{\mu_1\mu_2\mu_3}(p_1, p_2, p_3) =\ & H_1^{3g}(p^2) \ (\delta_{\mu_1\mu_2}(p_1 - p_2)_{\mu_3} + \text{cyclic permutations}) \\
& - H_2^{3g}(p^2)/p^2 \ (p_2 - p_3)_{\mu_1}(p_3 - p_1)_{\mu_2}(p_1 - p_2)_{\mu_3} \\
& + H_3^{3g}(p^2)/p^2 \ \left(p_{1_{\mu_3}} p_{2_{\mu_1}} p_{3_{\mu_2}} - p_{1_{\mu_2}} p_{2_{\mu_3}} p_{3_{\mu_1}} \right)
\end{aligned}
\qquad (7)
$$

with the momentum routing and indices as given in fig. 4.

We are interested in the limit $p^2 \to 0$ where the ghost-gluon vertex becomes bare again [24], $\Gamma_\mu^{gh}(p, q) = iq_\mu$ with q_μ being the momentum of the outgoing ghost. Substituting the power laws, eqs. (3), for the ghost and gluon dressing functions and employing (5) the IR behavior of the dressing functions H_1^{3g}, H_2^{3g} and H_3^{3g} of the vertex is determined analytically to be
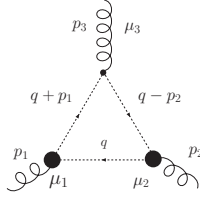
5

Fig. 4. Momentum routing in the ghost-loop diagram of the three-gluon vertex. All external momenta flow into the loop. Internal propagators are fully dressed.

$$H_1^{3g}(p^2) = -h(\kappa)\,\frac{1}{36}\,(\ 97\kappa^2 - 205\kappa + 100)\ (p^2)^{(-3\kappa)} \tag{8}$$

$$H_2^{3g}(p^2) = \ \ h(\kappa)\,\frac{2}{27}\,(\ 59\kappa^2 - 131\kappa + \ 56)\ (p^2)^{(-3\kappa)} \tag{9}$$

$$H_3^{3g}(p^2) = \ \ h(\kappa)\,\frac{1}{18}\,(119\kappa^2 - 323\kappa + 164)\ (p^2)^{(-3\kappa)} \tag{10}$$

with

$$h(\kappa) = \frac{-g^2 N_c B^3}{32\pi^2}\,\frac{\Gamma(3\kappa)\Gamma(1-2\kappa)\Gamma(1-\kappa)}{\Gamma(1+\kappa)\Gamma(2+2\kappa)\Gamma(3-3\kappa)} \tag{11}$$

and B being the leading IR coefficient of the ghost. Crucial to these expressions are the momentum power laws. All three dressing functions are proportional to $(p^2)^{(-3\kappa)}$, $i.e.$ with $\kappa > 0$ [28] the three-gluon vertex is IR singular, and the first of eqs. (4) is established. Note that the degree of singularity is the same for all three dressing functions, and given by three times $-\kappa$, the latter being the IR exponent of the ghost propagator. In the following it will become evident that the IR anomalous dimension of a diagram is simply the sum of IR exponents of propagators and vertices constituting the diagram. All trivial dimensions of the vertex are due to the tensor structure whereas the dressing functions H_1^{3g}, H_2^{3g} and H_3^{3g} are dimensionless. Any anomalous dimension appearing in the diagram of fig. 4 via nontrivial vertex or propagator dressings therefore has to appear in the functions H_1^{3g}, H_2^{3g} and H_3^{3g}. Therefore we can determine the degree of divergence of Greens functions just by counting IR anomalous dimensions. As p^2 is the only scale, $(p^2)^\rho$ with $\rho = -3\kappa$ has necessarily to arise in this case.

Note that a dressed ghost-gluon vertex would not have changed the running of H_1^{3g}, H_2^{3g} and H_3^{3g} with momentum, since in Landau gauge it carries no overall anomalous dimension. IR corrections to the vertex dressings can therefore be typically expressed as quotients p^n/q^n [9]. Such dressings cannot change the momentum dependence in eqs. (8-10). The following observation is important: The diagram in fig. 4 becomes IR singular if and only if all three incoming momenta $(p_1)^2, (p_2)^2$ and $(p_3)^2$ approach zero. This can be proven in general kinematics.[2] A convenient kinematic section to see this directly is $e.g.$ pro-

---

[2] Using appropriate projectors to single out the scalar dressing functions of the vertex one always ends up with scalar 'massless' triangle integrals with nontrivial powers of internal momenta. These integrals can be performed along the methods
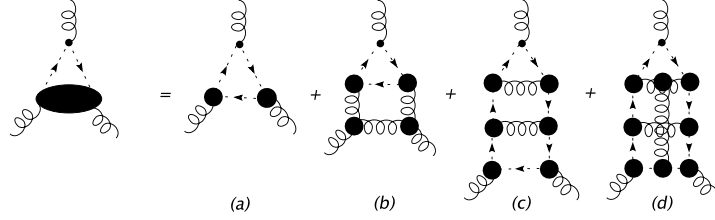
Fig. 5. Typical terms of the skeleton expansion of the ghost-gluon scattering kernel in the DSE for the three-gluon vertex. Internal propagators are fully dressed.

vided by $p_1^2 = $ constant, $p_2 = bp_1$ with b a constant that we will allow to approach zero. Due to momentum conservation the three momenta are then collinear and only one of them is small. With a convenient choice for the tensor basis, the leading coefficient calculated from the ghost triangle graph is

$$H_1^{3g} = \frac{g^2 N_c}{2} (\tilde{Z}_1)^3 \int \frac{d^4 k}{(2\pi)^4} \frac{b(b-3)(k^2 p_1^2 - k \cdot p_1^2) + (b-1)2k^2 k \cdot p_1}{6 p_1^2 (b^2 - 3b + 3)}$$
$$\frac{G(k^2)}{k^2} \frac{G((k+bp_1)^2)}{(k+bp_1)^2} \frac{G((k-p_1)^2)}{(k-p_1)^2} . \qquad (12)$$

In the limit $b \to 0$ the integrand is singular but integrable, and thus the corresponding diagram yields a finite contribution.

In the DSE for the three-gluon vertex no other term in the skeleton expansion has a larger power IR divergence. To show this we count powers for the remaining diagrams in fig. 3 and compare the result with eqs. (8-10). Employing eqs. (3-4) and denoting the remaining four diagrams as $(b) - (e)$, c.f. fig. 3, we obtain their IR anomalous dimensions by summing up the anomalous dimensions of all propagators and vertex functions of a diagram. Hereby a gluon propagator contributes an anomalous dimension of 2κ, a ghost propagator one of $(-\kappa)$, the three-gluon vertex one of (-3κ) and the ghost-gluon vertex carrys zero anomalous dimensions, c.f. eqs. (3) and (4). This yields for their respective IR exponents ρ:

(b) $\rho = 3 \times 2\kappa + 2 \times (-3\kappa) = 0,$ (c) $\rho = 5 \times 2\kappa + 3 \times (-3\kappa) = \kappa,$
(d) $\rho = 2 \times 2\kappa + 1 \times (-3\kappa) = \kappa,$ (e) $\rho = 2 \times 2\kappa + 1 \times (-3\kappa) = \kappa.$ (13)

Thus they are all subleading if compared to the ghost triangle diagram (a).

Finally we investigate further terms from the skeleton expansion. Typical corrections to the ghost-triangle diagram are given in fig. 5. The only scale appearing in the symmetric momentum kinematics is (p^2), thus we can determine the degree of divergence of the diagrams by counting anomalous dimensions.

---

described in refs. [30,31]. As we have checked explicitly, no IR singularities arise unless all three squared momenta vanish.
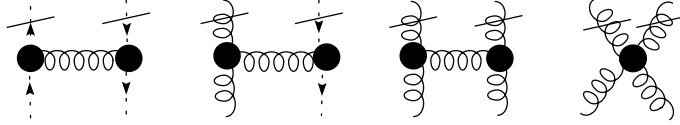
Fig. 6. Insertions generating the loop expansion in fig. 5. One should also allow for the possibility of upgrading a three to a four gluon vertex.

Denoting the higher order diagrams by $(b) - (d)$ we obtain for their IR anomalous dimensions

$$
\begin{aligned}
(b) \quad & \rho = (3 \cdot 2 + 3 \cdot (-1) + 2 \cdot (-3)) \, \kappa = -3\kappa, \\
(c) \quad & \rho = (2 \cdot 2 + 7 \cdot (-1)) \, \kappa = -3\kappa, \\
(d) \quad & \rho = (4 \cdot 2 + 8 \cdot (-1) + 1 \cdot (-3)) \, \kappa = -3\kappa,
\end{aligned}
\tag{14}
$$

with no contribution from the ghost-gluon vertex, as discussed above. Thus all these diagrams contribute to the same IR order as the ghost-loop diagram (a).

Arbitrary diagrams in the expansion can be generated with the four elements in fig. 6, by repeated insertion into a given lowest-order diagram. According to our counting rules based on eqs. (3) and (4) these insertions carry an overall zero IR anomalous dimension. Therefore in general, starting from a given diagram in the skeleton expansion with an IR anomalous dimension ρ all possible insertions generate diagrams of the next order in the skeleton expansion with the same degree of divergence. By induction this is true for the whole series of skeleton diagrams up to any order. *Therefore the degree of IR divergence of a fully dressed Greens function in the presence of only one external scale can be already read off by counting the anomalous dimensions of the lowest order diagrams in the skeleton expansion.* This general rule especially implies that higher order corrections to the diagrams $(b) - (e)$ of fig. 3 are all IR subleading. Thus the IR exponent $\rho = -3\kappa$ for the three-gluon vertex is established. [3]
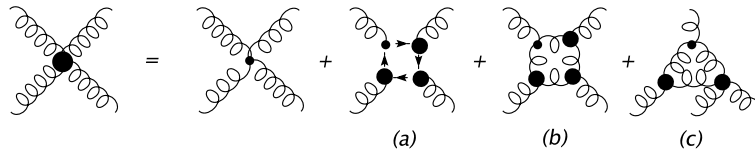

Fig. 7. First order expansion of the DSE for the four-gluon correlation. Internal propagators are to be understood as fully dressed.

The lowest order terms in the skeleton expansion of the DSE for the four-gluon vertex are given in fig. 7. Here we consider the special momentum configuration where all four momenta flowing into the loop are equal in magnitude and

---

[3] This result has been anticipated in [32] employing the STI $Z_1(\mu) = Z_3(\mu)/\tilde{Z}_3(\mu)$. In the presence of only one momentum scale all renormalized dressing functions run with $(p^2/\mu^2)^\alpha$, where α is the corresponding anomalous dimension. Therefore the IR powers in Eq.(3) imply that $Z_1(\mu) \sim (\mu^2)^{3\kappa}$ and $\rho = -3\kappa$ follows directly.

pairwise parallel or antiparallel. Denoting the ingoing momenta with $p_{i=1...4}$ we have $p_1^2 = p_2^2 = p_3^2 = p_4^2 \equiv p^2$ and all three Mandelstam variables $s = (p_1+p_2)^2$, $t = (p_2 + p_3)^2$ and $u = (p_1 + p_3)^2$ are either zero or proportional to p^2. With the IR counting rules established above we can then determine the degree of divergence of the three one-loop diagrams (a), (b) and (c). We obtain

$$(a) \ \rho = -4\kappa, \qquad (b) \ \rho = (4 \cdot 2 + 3 \cdot (-3)) \, \kappa = -\kappa,$$
$$(c) \ \rho = (3 \cdot 2 + 1 \cdot (-3) + 1 \cdot (-4)) \, \kappa = -\kappa. \tag{15}$$

Here the ghost box diagram is IR dominating, and yields -4κ as IR exponent for the four-gluon vertex.

Finally, we have to check whether eqs. (3) remain valid assuming the new results for the gluon-selfinteraction vertices. We therefore reconsider the DSE for the gluon propagator given diagramatically in fig. 8. Again due to the denominators of the propagators all diagrams are dominated by loop momenta similar to the external scale p^2. We can thus determine the IR behaviour for each diagram by the counting rules developed above. Note that the tadpole diagram contains only the bare four-gluon vertex and is independent of the external momentum.[4] For the other diagrams we obtain the following degree of IR divergence:

$$(a) \ \rho = -2\kappa, \quad (b) \ \rho = \kappa, \quad (c) \ \rho = 2\kappa, \quad (d) \ \rho = 2\kappa. \tag{16}$$

Clearly, the ghost-loop diagram is the leading diagram in the IR, and the analysis leading to eqs. (3) is thus not altered.

With analogous techniques one can straightforwardly prove that the generic IR behaviour of a $2n$-ghost–m-gluon amputated and connected Greens function is given by $(p^2)^{(n-m)\kappa}$.

To summarize this part, assuming that skeleton expansions of higher n-point Greens functions are well-defined we have shown:
• The degree of nonperturbative IR divergence of an n-point function is given already by the highest degree of divergence present in the lowest order skeleton expansion of the diagrams appearing in its DSE.
• In Landau gauge Yang-Mills theory the three-gluon vertex behaves as $(p^2)^{-3\kappa}$ and the four-gluon vertex as $(p^2)^{-4\kappa}$ in the IR.

A consistency check on this IR behaviour is, of course, given by its implication on the IR value of the running coupling as infered from these vertex functions. As we will see, these results allow for universality of the IR fixed point in Yang-Mills theory. A nonperturbative expression for the running coupling has been

---

[4] The tadpole diagram can even be completely absorbed in the renormalization.
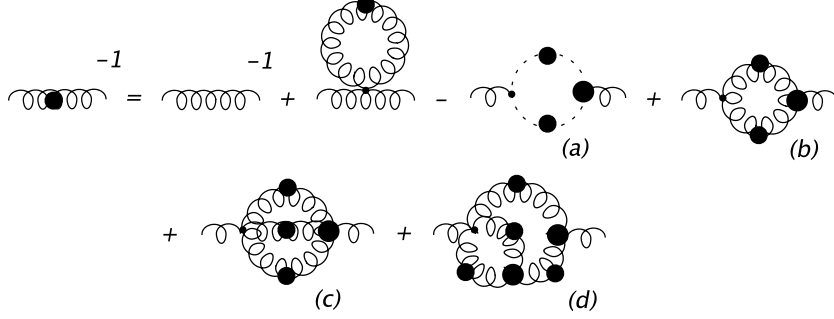
Fig. 8. The Dyson-Schwinger equation for the gluon propagator.

derived in the context of DSEs from the ghost-gluon vertex [6]. The Slavnov-Taylor identity (STI)

$$\widetilde{Z}_1 = Z_g \, \widetilde{Z}_3 \, Z_3^{1/2}, \tag{17}$$

relates the vertex renormalization factor $\widetilde{Z}_1$ with the corresponding factor Z_g for the coupling g and the ghost and gluon fields, $\widetilde{Z}_3^{1/2}$, $Z_3^{1/2}$. With the definition $\alpha = g^2/(4\pi)$ and the relation $g(\Lambda^2) = Z_g(\mu^2, \Lambda^2)g(\mu^2)$ one obtains

$$\alpha(\mu^2) = \alpha(\Lambda^2)\frac{\widetilde{Z}_3^2(\mu^2, \Lambda^2)Z_3(\mu^2, \Lambda^2)}{\widetilde{Z}_1^2(\mu^2, \Lambda^2)} \tag{18}$$

for the renormalized coupling at the renormalization point μ^2. The bare coupling $\alpha(\Lambda^2)$ depends on a regulator Λ^2. Since the ghost-gluon vertex is finite in Landau gauge, one may choose $\widetilde{Z}_1 = 1$. The bare and renormalized ghost and gluon dressing functions are related by

$$G_0(p^2, \Lambda^2) = G(p^2, \mu^2)\widetilde{Z}_3(\mu^2, \Lambda^2) \,, \quad Z_0(p^2, \Lambda^2) = Z(p^2, \mu^2)Z_3(\mu^2, \Lambda^2) \,. \tag{19}$$

Substituting these relations into eq.(18) we obtain

$$\alpha(\mu^2)G^2(p^2, \mu^2)Z(p^2, \mu^2) = \alpha(\Lambda^2)G_0^2(p^2, \Lambda^2)Z_0(p^2, \Lambda^2) \,. \tag{20}$$

Note that the r.h.s. is independent of μ^2 and thus the l.h.s. is renormalization group invariant [29]. Evaluating the l.h.s. once at an arbitrary renormalization point μ^2 and once at $\mu^2 = p^2$ we obtain

$$\alpha(p^2) = \alpha(\mu^2)G^2(p^2, \mu^2)Z(p^2, \mu^2) \tag{21}$$

where we have exploited the renormalization condition $G^2(p^2, p^2)Z(p^2, p^2) = 1$ for the renormalized dressing functions. Evaluating $\alpha(p^2)$ in the ultraviolet one recovers the well known perturbative coupling in the MOM-scheme which can be related to the $\overline{MS}$-coupling by standard techniques [14].

The IR behaviour of this coupling can be read off from the power law behaviour of the ghost and gluon dressing functions in eqs. (3). Due to the interrelated exponents in these expressions the IR momentum dependence cancels and

10

leads to a fixed point at $p^2 = 0$. The precise value of $\alpha(0)$ depends on κ. It has been calculated in both, DSEs and ERGEs, employing several kinds of truncation schemes [6,7,8,9,10,18,19]. Neglecting IR corrections from the dressing of the ghost-gluon vertex yields

$$\alpha(0) = \frac{2\pi}{3\,N_c} \frac{\Gamma(3-2\kappa)\Gamma(3+\kappa)\Gamma(1+\kappa)}{\Gamma^2(2-\kappa)\Gamma(2\kappa)} \approx 8.915/N_c \,. \tag{22}$$

For the running coupling based on the three-gluon vertex we employ the STI

$$Z_1 = Z_g\, Z_3^{3/2} \tag{23}$$

relating the renormalization factor of the three-gluon vertex to the one of the coupling and the gluon fields. The vertex renormalization factor Z_1 relates the regularized and the renormalized three-gluon vertex via

$$\Gamma^{\mu\nu\lambda}(p_1,p_2,p_3,\mu^2) = \Gamma_0^{\mu\nu\lambda}(p_1,p_2,p_3,\Lambda^2)\, Z_1(\mu^2,\Lambda^2) \,. \tag{24}$$

Evaluating the vertex at the symmetric point $p_1^2 = p_2^2 = p_3^2 \equiv p^2$ one obtains

$$H_1^{3g}(p^2,\mu^2) = H_1^{3g}(p^2,\Lambda^2)\, Z_1(\mu^2,\Lambda^2) \tag{25}$$

and thus a relation between the renormalized and the regularized H_1^{3g} as defined in eq. (7). One can also derive an expression for the three-gluon coupling:

$$\alpha^{3g}(p^2) = \alpha_0^{3g}(\mu^2)\,(H_1^{3g})^2(p^2,\mu^2)\,Z^3(p^2,\mu^2) \tag{26}$$

where we exploited the renormalization condition $(H_1^{3g})^2(p^2,p^2)Z^3(p^2,p^2) = 1$. This condition involves only H_1^{3g} because it multiplies the tensor structure of the three-gluon vertex containing the primitive UV divergence. Again the r.h.s. of this equation denotes an RG invariant quantity. This coupling is related to the one of the ghost-gluon vertex by a known scale transformation [14].

Recalling that $H_1^{3g}(p^2) \sim (p^2)^{-3\kappa}$ and $Z(p^2) \sim (p^2)^{2\kappa}$ we obtain

$$\alpha^{3g}(p^2 \to 0) \sim const./N_c \,, \tag{27}$$

i.e. the running coupling taken from the three-gluon vertex possesses an IR fixed point in accordance with the coupling determined from the ghost-gluon vertex. The explicit $1/N_c$-dependence stems from the fact that $g^2 \sim 1/N_c$ and the functions H_1^{3g} and Z are independendent of N_c, as can be seen from their DSEs. Note that also other renormalization conditions for the three-gluon vertex involving H_2^{3g} and H_3^{3g} are possible [14]. The expression (26) for the coupling would then include a corresponding linear combination of the functions H_1^{3g}, H_2^{3g} and H_3^{3g}. All of these functions are proportional to $(p^2)^{-3\kappa}$ in the IR, therefore such a redefinition of the coupling would not affect the presence of the IR fixed point.

Finally we examine the four-gluon coupling. Its STI is $Z_4 = Z_g^2 Z_3^2$, and thus we obtain the relation

$$H_1^{4g}(p^2, \mu^2) = H_1^{4g}(p^2, \Lambda^2) \; Z_4(\mu^2, \Lambda^2) \; . \tag{28}$$

The running coupling from the four-gluon vertex is therefore given by

$$\alpha^{4g}(p^2) = \alpha_0^{4g}(\mu^2) \; H_1^{4g}(p^2, \mu^2) \; Z^2(p^2, \mu^2) \tag{29}$$

where analogously to the three-gluon vertex case the renormalization condition $H_1^{4g}(p^2, p^2) Z^2(p^2, p^2) = 1$ has been employed. Recalling that $H_1^{4g}(p^2) \sim (p^2)^{-4\kappa}$ and $Z(p^2) \sim (p^2)^{2\kappa}$ in the IR we again obtain an IR fixed point,

$$\alpha^{4g}(p^2 \rightarrow 0) \sim const./N_c. \tag{30}$$

To summarize, we have demonstrated on a qualitative level that the running couplings from the ghost-gluon, three-gluon and four-gluon vertices have a universal, nontrivial fixed point in the IR. The value of the fixed point for the ghost-gluon coupling is known to depend slightly on the IR dressing of the ghost-gluon vertex and falls into a small window $2.5 < \alpha(0) < 3$ for $N_c = 3$ [9]. The corresponding value for the other couplings can be calculated from the vertex-DSEs. In the skeleton expansion the dressed three- and four-gluon vertices receive their IR leading contributions from an infinite number of diagrams belonging to a certain subclass. These can be constructed from the ghost-triangle diagram by repeated insertion of the diagrammatic pieces given in fig. 6. In the IR, all these diagrams have the same dependence on one external momentum scale. In principle, the momentum independent coefficients can be calculated order by order in the skeleton expansion, although its convergence properties are yet to be determined. The nonperturbative expressions for the three- and four-gluon vertices are IR singular provided all external squared momenta approach zero. This singularity, however, is not strong enough to compensate the zeroes in the gluon dressing functions of attached gluon propagators. Thus in the skeleton expansion of all DSEs the ghost-loop diagrams are leading in the IR. This is in agreement with a picture recently advocated by Zwanziger [13]: the geometric degrees of freedom, *i.e.* the Faddeev-Popov determinant, dominate IR Yang-Mills theory.

References

[1] F. D. Bonnet *et al.*, Phys. Rev. D **64** (2001) 034501.

[2] K. Langfeld, H. Reinhardt and J. Gattnar, Nucl. Phys. B **621** (2002) 131.

[3] P. O. Bowman, U. M. Heller, D. B. Leinweber, M. B. Parappilly and A. G. Williams, Phys. Rev. D **70** (2004) 034509.

[4] P. J. Silva and O. Oliveira, Nucl. Phys. B **690** (2004) 177.

[5] R. Alkofer and L. von Smekal, Phys. Rept. **353** (2001) 281.

[6] L. von Smekal, R. Alkofer and A. Hauck, Phys. Rev. Lett. **79** (1997) 3591; L. von Smekal, A. Hauck and R. Alkofer, Annals Phys. **267** (1998) 1.

[7] D. Atkinson and J. C. Bloch, Mod. Phys. Lett. A **13** (1998) 1055; Phys. Rev. D **58** (1998) 094036.

[8] D. Zwanziger, Phys. Rev. D **65** (2002) 094039.

[9] C. Lerche and L. von Smekal, Phys. Rev. D **65** (2002) 125006.

[10] C. S. Fischer and R. Alkofer, Phys. Lett. **B536** (2002) 177; C. S. Fischer, R. Alkofer and H. Reinhardt, Phys. Rev. **D65** 2002 094008; R. Alkofer, C. S. Fischer and L. von Smekal, Acta Phys. Slov. **52** (2002) 191; C. S. Fischer, PhD thesis, U. of Tuebingen, arXiv:hep-ph/0304233.

[11] R. Alkofer, W. Detmold, C. S. Fischer and P. Maris, Phys. Rev. D **70** (2004) 014014; arXiv:hep-ph/0411367.

[12] T. Kugo, Int. Symp. on BRS symmetry, Kyoto, Sep. 18-22, 1995, arXiv:hep-th/9511033.

[13] D. Zwanziger, Phys. Rev. D **69** (2004) 016002.

[14] W. Celmaster and R. J. Gonsalves, Phys. Rev. D **20** (1979) 1420.

[15] D. V. Shirkov and I. L. Solovtsov, Phys. Rev. Lett. **79** (1997) 1209.

[16] I. L. Solovtsov and D. V. Shirkov, Theor. Math. Phys. **120** (1999) 1220 [Teor. Mat. Fiz. **120** (1999) 482].

[17] D. M. Howe and C. J. Maxwell, Phys. Rev. D **70** (2004) 014002.

[18] J. M. Pawlowski, D. F. Litim, S. Nedelko and L. von Smekal, Phys. Rev. Lett. **93** (2004) 152002.

[19] C. S. Fischer and H. Gies, JHEP 0410 (2004) 048.

[20] P. M. Stevenson, Phys. Rev. D **23** (1981) 2916.

[21] S. J. Brodsky, G. P. Lepage and P. B. Mackenzie, Phys. Rev. D **28** (1983) 228.

[22] F. J. Llanes-Estrada and S. R. Cotanch, arxiv:nucl-th/0408038; F. J. Llanes-Estrada *et al.*, Phys. Rev. C**70** (2004) 035202.

[23] D. Zwanziger, Phys. Lett. B **257** (1991) 168.

[24] J. C. Taylor, Nucl. Phys. B **33** (1971) 436.

[25] W. J. Marciano and H. Pagels, Phys. Rept. **36** (1978) 137.

[26] W. Schleifenbaum, A. Maas, J. Wambach and R. Alkofer, arXiv:hep-ph/0411052.

[27] A. Cucchieri, T. Mendes and A. Mihara, arXiv:hep-lat/0408034.

[28] P. Watson and R. Alkofer, Phys. Rev. Lett. **86** (2001) 5239.

[29] S. Mandelstam, Phys. Rev. D **20** (1979) 3223.

[30] E. E. Boos and A. I. Davydychev, Theor. Math. Phys. **89** (1991) 1052 [Teor. Mat. Fiz. **89** (1991) 56].

[31] C. Anastasiou, E. W. N. Glover and C. Oleari, Nucl. Phys. B **572** (2000) 307.

[32] P. Watson, Ph.D thesis, University of Durham, UK, 2000.